## Title

ANALYSIS OF THE OPTICAL SPECTRUM OF Np(BD4)4 DILUTED IN Zr(BD4)4 AND THE MAGNETIC PROPERTIES OF Np(BH4)4 AND Np(BH3CH3)4



## Author

Rajnak, K.

## Publication Date

1983-09-01

# Lawrence Berkeley Laboratory
UNIVERSITY OF CALIFORNIA



## Materials & Molecular Research Division

Submitted to the Journal of Chemical Physics

# ANALYSIS OF THE OPTICAL SPECTRUM OF $Np(BD_4)_4$ DILUTED IN $Zr(BD_4)_4$ AND THE MAGNETIC PROPERTIES OF $Np(BH_4)_4$ AND $Np(BH_3CH_3)_4$

K. Rajnak, R.H. Banks, E. Gamp, and N. Edelstein

September 1983



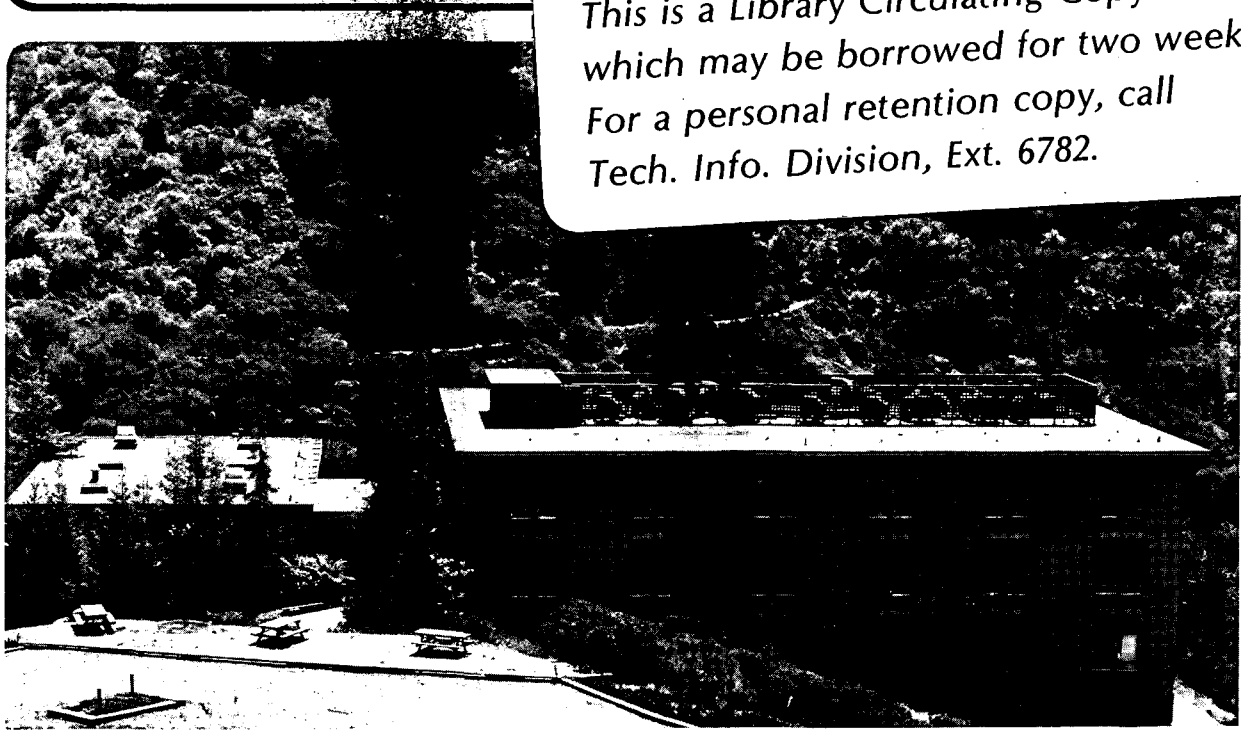

Prepared for the U.S. Department of Energy under Contract DE-AC03-76SF00098

## DISCLAIMER

LBL-16486

# Analysis of the Optical Spectrum of $Np(BD_4)_4$ Diluted in $Zr(BD_4)_4$ and the Magnetic Properties of $Np(BH_4)_4$ and $Np(BH_3CH_3)_4$[a]

K. Rajnak,* R. H. Banks**, E. Gamp, and N. Edelstein

Materials and Molecular Research Division
Lawrence Berkeley Laboratory
University of California
Berkeley, California 94720

## Abstract

The optical spectrum of $Np(BD_4)_4/Zr(BD_4)_4$ is reported and analyzed. The parameter values obtained are consistent with those for $U(BD_4)_4/Hf(BD_4)_4$ (J. Chem. Phys., previous paper). A total of 46 levels were fit with $\sigma = 84$ cm$^{-1}$. EPR data on $Np(BD_4)_4/Zr(BD_4)_4$ and $Np(BH_3CH_3)_4/Zr(BH_3CH_3)_4$ and the magnetic susceptibility of $Np(BH_3CH_3)_4$ are reported. They could be fit with the eigenvectors from the optical analysis only by the inclusion of orbital reduction factors $k = 0.885$ for $Np(BD_4)_4$ and 0.862 for $Np(BH_3CH_3)_4$. These values indicate greater covalency for the methylborohydride.

## Introduction

At room temperature Np borohydride is a volatile, reactive liquid whose physical properties closely resemble those of Hf and Zr borohydrides rather than its neighbor in the periodic table,

$U(BH_4)_4$. It is monomeric in the solid state, and the local symmetry about the $Np^{4+}$ ion is $T_d$.[1] This high symmetry plus the $5f^3$ electron configuration makes $Np(BH_4)_4$ an attractive candidate for magnetic and optical studies. In addition, our reanalysis[2] of Bernstein and Keiderling's spectra[3] of $U(BD_4)_4$ diluted in $Hf(BD_4)_4$ provides initial values for the crystal field parameters. In this paper we report detailed measurements and the analysis of the optical spectra of $Np(BD_4)_4$ diluted in $Zr(BD_4)_4$ as well as EPR measurements on this system. We also compare the average spin-Hamiltonian parameters of the closely related molecule $Np(BH_3CH_3)_4$ diluted in $Zr(BH_3CH_3)_4$ and report the measurement of the magnetic susceptibility of $Np(BH_3CH_3)_4$ from approximately 2 K - 300 K. In the following paper[4] a complete analysis of the unexpectedly anisotropic EPR spectra of $Np(BH_3CH_3)_4$ diluted in single crystals of $Zr(BH_3CH_3)_4$ is given.

## Experimental

The preparation and purification of $Np(BH_4)_4$, $Zr(BH_4)_4$, their deuterated analogs, $Np(BH_3CH_3)_4$, and $Zr(BH_3CH_3)_4$ have been described previously.[1,5] Single crystals of pure $Np(BH_4)_4$ or $Np(BD_4)_4$ were grown by simply cooling the liquid (at room temperature) very slowly in a quartz cell placed in an optical dewar. When the sample temperature reached ~ 150 K, in approximately 8 hours, liquid helium was added which was subsequently

pumped below the lambda point. All spectra given in this paper were recorded on a Cary 17 spectrophotometer with the sample at ~ 2 K. Mixed crystals of $Np(BH_4)_4/Zr(BH_4)_4$ and $Np(BD_4)_4/Zr(BD_4)_4$ were grown from the vapor following the method of Bernstein and Keiderling.[3]

Spectra were also obtained with $Np(BH_4)_4$ or $Np(BD_4)_4$ isolated in a methylcyclohexane glass. These spectra were similar to those obtained in single crystals but had larger linewidths. In the photographic region, 300-900 nm, low temperature spectra of $Np(BD_4)_4/Zr(BD_4)_4$ were obtained on a 3/4 m Jarrell-Ash spectrograph with higher resolution than the Cary 17. No additional structure was observed.

For EPR measurements, approximately 50-100 mg of $Zr(BH_4)_4$ or $Zr(BD_4)_4$ were transferred to the bottom of a 3 mm ID quartz EPR tube. A small amount (~ 100 μg) of $Np(BH_4)_4$ or $Np(BD_4)_4$ was then condensed onto the Zr compound. Due to the size of the microwave cavities, the sample tubes could be no longer than 3 cm. The seal-off area on the quartz tube was kept at ~ 100 C during the transfer of the borohydrides by heating a nichrome wire wrapped around the area in order to prevent mirror formation on the tube (which appreciably lowered the cavity Q). The sample was held at 77 K during the seal off operation. The solid borohydride mixture was then melted to give a solution whose green color was barely perceptible. Following solidification of the liquid at one end of the tube, the other end was kept immersed in 1/4 in. of ice water for 15 hours. The resulting

vapor-grown single crystal was homogeneous and transparent.

The EPR measurements at X and Q bands were made at 4.2 K with Varian models E-101 (9 GHz) and E-110 (34.5 GHz) microwave bridges. The magnetic field was produced by a rotating electromagnet with a 2-5/8" gap (12" diameter polefaces, maximum field strength 10.8 kG) and measured with an Alpha Scientific NMR gaussmeter monitored by a frequency counter. K band spectra were obtained with a superheterodyne spectrometer at 1.7 K in the region 24-25 GHz. A George Associates rotating-coil gaussmeter was used to measure the magnetic field.

For the later experiments at 35 GHz on $Np(BH_3CH_3)_4$ samples, the magnet pole faces were changed so that a field of 16 kG could be obtained with a gap of 2". The preparation of single crystals of $Np(BH_3CH_3)_4$ diluted in $Zr(BH_3CH_3)_4$ and of $Np(BH_3CH_3)_4$ in a methylcyclohexane glass are described in the following paper.[4]

Magnetic susceptibility measurements were carried out as described previously.[2] One sample of $Np(BH_3CH_3)_4$ was measured with a nominal weight of 10 mg. Because of problems of obtaining an accurate weight on this small sample, the weight of the sample was adjusted so that the susceptibilities at low temperature agreed with the values calculated from the g value obtained by EPR measurements.

## Results

Optical spectra of $Np(BD_4)_4/Zr(BD_4)_4$, $Np(BD_4)_4$,

$Np(BH_4)_4/Zr(BH_4)_4$, and $Np(BH_4)_4$ are shown in Figures 1 and 2. The $Np(BD_4)_4/Zr(BD_4)_4$ spectra have the narrowest linewidths and were chosen for a detailed analysis. Blanks were run on the Zr host crystals so as to be able to distinguish pure vibrational overtones from electronic and electronic plus vibrational transitions.

The EPR spectra for single crystals of $Np(BH_4)_4/Zr(BH_4)_4$ and $Np(BD_4)_4/Zr(BD_4)_4$ were isotropic and could be fit to the parameters of the spin-Hamiltonian

$$H = g\beta \underline{H} \cdot \underline{S}' + A\underline{I} \cdot \underline{S}' \qquad (1)$$

where the effective spin $S' = 1/2$, the nuclear spin $I = 5/2$ for the $^{237}Np$ nucleus, $\beta$ is the Bohr magneton, g the g value, H the applied magnetic field, and A the hyperfine coupling constant. The values of g and A are given in Table I. The EPR spectrum of pure $Np(BD_4)_4$ consisted of one broad line (linewidth ~ 5000 gauss) centered at $g = 2.0 \pm .2$.

The EPR spectra of $Np(BH_3CH_3)_4$ diluted in $Zr(BH_3CH_3)_4$ were slightly anisotropic. However, for $Np(BH_3CH_3)_4$ dissolved in methylcyclohexane, an isotropic resonance was observed with the spin-Hamiltonian parameters shown in Table I. A detailed presentation and analysis of the data for the diluted crystal are given in the following paper. The average values of g and A for that system are given in Table I.

Table I shows the hyperfine coupling constant as 0.114 $cm^{-1}$. Because this constant is so large, we cannot make the usual assumption that the Zeeman term (the first term on the right hand side of Eq. (1)) is large compared to the hyperfine term. In order to fit the experimental spectra to the parameters of the spin Hamiltonian, the exact energies obtained from the Breit-Rabi equation,[6] were used. In fact at X-band frequencies, ~ 9.4 GHz, the zero field splitting, 3A, was greater than the microwave energy, so that only four transitions were observed. The spectra at X-band and at 24 GHz are shown in Figure 3. The energy level diagram showing the various transitions is given in Figure 4.

For a $5f^3$ ion, a J = 9/2 multiplet will lie lowest. In $T_d$ symmetry this multiplet splits into one $\Gamma_6$ and two $\Gamma_8$ states. The $\Gamma_8$ states should show anisotropic behavior in a magnetic field so we assign the observed EPR resonances to the isotropic $\Gamma_6$ state. This fixes the symmetry of the ground crystal field state for the following optical analysis.

The reciprocal of the magnetic susceptibility of pure $Np(BH_3CH_3)_4$ vs. temperature is shown in Figure 5. Considering only the $^4I_{9/2}$ ground term (a bad approximation), curve A was obtained with crystal field parameters, $B_0^4 = -1460.7\ cm^{-1}$, $B_0^6 = -3274.4\ cm^{-1}$, and the orbital reduction factor k = 0.82.

Optical Analysis

The absorption lines of $Np(BD_4)_4/Zr(BD_4)_4$ are given in

Table II. The vibrational energies of $Np(BD_4)_4$ have been determined from the IR and Raman spectra.[7,8] Table III shows the corresponding energies of vibrations associated with the various origins as identified in this analysis. The assignments for some of the lower levels are discussed in detail below. The designation of the vibrations is the same as that in the previous paper[2] which retained, insofar as possible, the notation of Bernstein and Keiderling.[3] Some vibrations appear here which were not clearly identified in the $U(BD_4)_4$ analysis. The data were analyzed with the same Hamiltonian[9,10] used for $U(BD_4)_4/Hf(BD_4)_4$, but with the addition of the 3-body configuration interaction parameters[11] $T^k$ which do not arise for $f^2$ configurations.

From the $\Gamma_6$ ground state found from the EPR measurements, transitions are allowed to both $\Gamma_7$ and $\Gamma_8$ states; all vibrations can couple with $\Gamma_8$ states and all but $T_2$ vibrations can couple with $\Gamma_7$'s. Since there is only one vibration with $T_2$ symmetry, this is not of much help in making assignments. Consequently, they were based on the following criteria:

1) the ability to assign a consistent set of vibrational energies associated with given origin;

2) agreement between calculated and experimental energies;

3) association of origins with sharp lines unless vibronics from another origin have nearly the same energy;

4) assignment of the strongest lines as origins unless that conflicted strongly with 1) and 2).

These criteria provide neither a clear distinction between origins and vibrations nor a unique association between origins and particular $\Gamma_7$ or $\Gamma_8$ states.

Somewhat more useful was the additional requirement that

5) the resultant parameter values bear expected relationships to those of $U(BD_4)_4$.

We expected the crystal field parameters of $U(BD_4)_4$ and $Np(BD_4)_4$ to be nearly the same. Two different approaches were taken to establishing an expected range of the free-ion parameters. Pseudo-relativistic Hartree-Fock (HFR) functions were calculated for $U^{4+}$ and $Np^{4+}$ with the code of Cowan and Griffin.[12] (See Table IV). It was assumed that the differences between the HFR values of $F^2$, $F^4$, $F^6$ and $\zeta$ and the values for the borodeuterides would be the same for both $U^{4+}$ and $Np^{4+}$. Since the $U^{4+}$ free ion spectra have been analyzed,[13] the same procedure can be used to estimate the free-ion parameters for $Np^{4+}$. The second approach to the borodeuteride parameters was the assumption that the differences between the $U(BD_4)_4$ and $Np(BD_4)_4$ parameter values would be the same as those found for $U^{3+}$ and $Np^{3+}$ substituted in $LaCl_3$[14] (Table V). These considerations led us to expect parameters for neptunium borodeuteride in the following ranges:

$F^2 = 44400 - 46500\ cm^{-1}$, $F^4 = 42069 - 43400\ cm^{-1}$

$F^6 = 24080 - 24600\ cm^{-1}$, $\zeta = 2065 - 2090\ cm^{-1}$ and to

predict $F^2 = 54463$ and $\zeta = 2253\ cm^{-1}$ for the $Np^{4+}$ free ion.

The preliminary results referred to previously[15] relied heavily on the assignment of the strongest lines as origins. About 30 levels could be fit with $\sigma \sim 80$ cm$^{-1}$ but criterion 5 was not satisfied. $B_0^4$ was $\sim -5000$ cm$^{-1}$ vs. $-2448$ for $U(BD_4)_4/Hf(BD_4)_4$. $F^2$ was $\sim 42000$ cm$^{-1}$, the same as for $U(BD_4)_4$ and much lower than expected.

Therefore we began again, changing some of the infrared assignments, fixing parameters where necessary to keep them in the right range, gradually adding levels until most of the parameters could be fit. Those levels which deviated most from the calculations were continually reexamined to see if another choice of origin could fit the calculation better and still allow reasonable assignment of the vibrations. With the close spacing of the levels and the large number of different vibrational frequencies, this was often possible. It did require, however, that in some cases the strongest line in a group be assigned as a vibronic transition rather than as an origin. The same was true for some $U(BD_4)_4$ transitions.

The final assignments given in Table II are certainly not unique, and they are not independent of the calculations. Some of the lower levels are discussed in detail below.

1) origin a, 5605 cm$^{-1}$

The differences in intensity of the vibronics involving various groups of vibrations are clearly seen in Fig. 1. The origin is followed by a strong group of lines involving a single phonon in the

100-200 $cm^{-1}$ energy range ($\beta$, $\delta$, and $\epsilon$ of Table III). These vibronics are nearly as sharp as the origin. The weak and broader transitions involving multiples of these phonons are followed by another strong, sharp group involving single phonons in the 400-500 $cm^{-1}$ energy range ($\zeta$, n', $\eta$, $\theta$). Weak transitions involving one phonon from each of the two groups are followed by another set of vibronics with single phonons of 800-950 $cm^{-1}$ ($\gamma$, $\chi$, $\Xi$, $\lambda$, $\lambda'$). The one-phonon vibronics with energies ~ 1500 $cm^{-1}$ ($\xi$, $\xi'$, $\xi''$) seen at ~ 1400 nm in Fig. 2 are almost as strong as the first group. One possible interpretation of the weak transitions at ~ 1180 nm is as vibronics involving two of these phonons.

The very weak broad peak immediately following the origin (designated xx in Tables II and III) is of too low a frequency to correspond to a vibration of the $Np(BD_4)_4$ molecule. It must be attributed to a lattice mode. A similar weak transition occurred in the $U(BD_4)_4/Hf(BD_4)_4$ spectrum although the energy was 114 $cm^{-1}$.

There is another vibrational energy, 138 $cm^{-1}$, designated xxx in Table III, which cannot be associated with any of the normal modes of the $Np(BD_4)_4$ molecule. This one is associated with a strong, sharp vibronic, however. It also appears coupled in multiphonon vibronics of origin a but is not associated with any other origins.

In the IR spectrum Banks and Edelstein[7] observed two vibrations at 437 and 457 $cm^{-1}$ which were assigned to the same vibrational mode, but the 457 $cm^{-1}$ vibration was associated with $^{10}B$ rather

than $^{11}B$. The $^{10}B$ vibration was weaker as expected from the relative abundances of $^{11}B$ and $^{10}B$. When associated with origin a, these energies are 430 and 452 $cm^{-1}$, but the higher energy one is much more intense. These vibrations are designated $\eta'$ and $\eta$ in Tables II and III. No attempt has been made to confirm the $^{10}B$ assignment. The two vibrations appear together only with origin a and the stronger one, $\eta$, is more frequently observed.

2) Origin b, 7083 $cm^{-1}$

As seen in Fig 2, this strong sharp line, which certainly looks like an origin, nearly disappears in the pure $Np(BD_4)_4$ spectrum. If we assign this line as a forbidden transition that has become allowed due to a slight lowering of the $T_d$ symmetry in the $Zr(BD_4)_4$ crystal, we have two problems: the isotropy of the ground state g value and the lack of evidence for two transitions. Many of our calculations placed $\Gamma_6$ and $\Gamma_8$ levels ~ 50 $cm^{-1}$ apart in this region with the $\Gamma_6$ lower. The $\Gamma_8$ assigned to this origin fit very poorly. If part of the intensity is due to a vibronic of the forbidden $\Gamma_6$ level, the separation between the $\Gamma_6$ and $\Gamma_8$ would be that of the $\beta$ or $\delta$-vibration, ~ 120 or ~ 160 $cm^{-1}$, instead of 50 $cm^{-1}$. Both levels would then fit very poorly in the calculations. The final calculation puts the $\Gamma_6$ and $\Gamma_8$ levels only 0.3 $cm^{-1}$ apart. Consequently, we cannot rule out the possibility that the two levels are very nearly degenerate and that the enhanced intensity in the dilute crystal is somehow related to

this fact.

As seen in Tables II and III most of the vibrations associated with origin a are associated with b also. A few of these have 10-15 $cm^{-1}$ differences in energy.

3) Origin c, 7594 $cm^{-1}$

We first assigned origin c as the very strong transition at 7690 $cm^{-1}$. It was possible to fit a group of 30 or 40 levels with this as one of the assignments, but the deviation of this level was always > 200 $cm^{-1}$ when $\sigma$ was ~ 100 $cm^{-1}$. When this level and the previous one were weighted 50 times as strongly as the others, it was again possible to obtain $\sigma$ ~ 100 $cm^{-1}$, now with these levels fitting very well, but with $F^4$ ~ 40000 and $B_0^4$ ~ -4700 $cm^{-1}$. These are both well outside the expected ranges.

A further reason for rejecting this strong line as an origin is the lack of strong vibronics associated with it. In general, the intensity of the electronic transition is reflected in at least the first vibronics. It is possible to assign five reasonable vibrational energies with this as an origin, but three of these are observed only in combinations.

If the transition at 7690 $cm^{-1}$ is to be assigned as a vibronic, the origin must be one of the sharp transitions at 7642 or 7694 $cm^{-1}$. The lower one is in better agreement with the calculations, but a larger number of vibronics can be assigned with the higher one as the origin. Furthermore, this transition has a less likely

explanation as a vibronic of b. Consequently, 7694 has been chosen as an origin. With this choice, all of the transitions up to 9000 $cm^{-1}$ can be assigned as vibronics associated with origins a, b, and c.

The strong transition at 7690 $cm^{-1}$ must be interpreted as a vibronic associated with the $\beta$ vibration (96 $cm^{-1}$) and/or the $\eta$ vibration associated with the $\Gamma_6$ level calculated at 7193 $cm^{-1}$. Some of the intensity of this line could also come from vibronics of origin b. The lack of an $\epsilon$ vibronic associated with c is consistent with its assignment as a $\Gamma_7$ level.

4) Origins d and e, 9281 and 9571 $cm^{-1}$

The next group begins with a weak but sharp line at 9281 $cm^{-1}$ which cannot be easily associated with a vibronic of origin c. It is the only line which is appreciably stronger in the pure than in the dilute crystal. The large number of one- and two-phonon vibronics which can be associated with it make this assignment (origin d) quite certain. The $\beta$ vibration is assigned to the sharp line at 9403 which is four times as intense. A similar intensity ratio for origin c and its $\beta$ vibronic would account for more than half of the intensity of the peak at 7690 $cm^{-1}$.

The assignment of origin e is less clear-cut. The strong line at 9449 $cm^{-1}$ could be all or partly due to the $\delta$ vibronic of d. If it is chosen as origin e, then the $\beta$ vibronic is the relatively strong line at 9571 $cm^{-1}$, but the $\delta$ is a very weak broad line better associated with multiple phonons. If 9571 $cm^{-1}$ is chosen as origin,

then the β and δ vibronics are both sharp and intense. This is more consistent with the assignment of those vibronics associated with other origins. Thus 9571 $cm^{-1}$ was chosen as the origin.

The strong sharp line at 10335 $cm^{-1}$ must then be explained as a sum of vibronics associated with origins d and e. The much lower intensity of this line in pure $Np(BD_4)_4$ is more consistent with such an interpretation. There is no way in which this line can be fit as an origin with parameters within the expected range.

5) Origin f, 10709 $cm^{-1}$

The most obvious choice of an origin in this region is the rather broad line at 10576 $cm^{-1}$, but it fits the calculations very poorly. That leaves either the line at 10709 or the one at 10796 $cm^{-1}$. Despite its width, we have chosen the former because of the impossibility of associating vibronics with the higher one. The width of the 10709 $cm^{-1}$ line can be explained by near coincidence with vibronics of d and e. The line at 10796 $cm^{-1}$ is well explained as the ξ vibronic of d.

6) Higher origins

The assignments of the strong origins g-n was fairly straightforward, but beyond 14000 $cm^{-1}$ the lines are less sharp and generally weak. Fewer and fewer vibronics are seen. This is associated with both the decreasing intensity and decreasing resolution. As we have assigned the levels, the more intense origins

generally do exhibit vibronics. But without the vibronics, the choice of origins is more ambiguous. Some of the sharp lines which look most like origins fit the calculations very poorly. This could be due either to erroneous identification as origins or to the breakdown of the crystal field model. A vibronic intensity analysis is needed to verify the assignments.

The final assignments are shown in Tables II and III. The parameters are given in Table V and the observed and calculated levels are compared in Table VI. The rms deviation $\sigma$ is 84 $cm^{-1}$ for 46 levels.

## Discussion

The observed levels cover less than half of the entire spread of the $5f^3$ configuration in this crystal and, without the higher levels, $F^4$ and $F^6$ cannot be uniquely determined. Likewise, the $T^k$, $P^k$ parameters and $\beta$ must be regarded as only very approximately determined. Attempts to fit $\beta$ or $T^2$ reduced $\sigma$ by only ~ 1 $cm^{-1}$.

In spite of this uncertainty in the free ion parameter values, it is clear that significant improvement in the fit cannot come from changes in these values; modification of the crystal field Hamiltonian appears to be necessary.

Already in $U^{4+}/ThBr_4$[16] where the crystal field is ~ 2.5 times smaller than in the borodeuterides, there was evidence for the breakdown of the crystal field model. The fit was worse for

$U(BD_4)_4/Hf(BD_4)_4$, but the large differences between experimental and calculated levels were still confined to relatively few states. For $Np(BD_4)_4$, however, levels which fit well are the exceptions. The higher density of states for $f^3$ increases J-mixing and seems to magnify the problems.

The borodeuteride data is probably not the place to test a new crystal field model, however. The large number of vibronic transitions gives rise to too many ambiguities in the identification of electronic origins. A new model should be tested in a system in which the levels are identified with more certainty. Of the currently available data, that for $U^{4+}/ThBr_4$ would probably be the best test case.

The parameter values shown in Table V are good enough to allow some tentative conclusions regarding relative covalency in $U(BD_4)_4/Hf(BD_4)_4$ and $Np(BD_4)_4/Zr(BD_4)_4$ and in the tetravalent vs. trivalent actinides. With few exceptions, for $d^N$ series fluorides in the same oxidation state covalency (as measured by decreases in the nephalauxetic ratio $\beta = B/B_{free\ ion}$) increases with increasing atomic number.[17] If the Racah parameters B and C are transformed to $F^k$'s, the effect is the same, i.e. $\phi_2 = F^2/F^2_{free\ ion}$ decreases with increasing Z. Although C is often poorly determined, the same effect is reflected in increasing ratios C/B or $r_{42} = F^4/F^2$ along a $d^N$ series. This measure has the advantage of not requiring knowledge of the free ion parameters. The results of Crosswhite et al.[14] show that, contrary to the $d^N$

series, $r_{42}$ decreases with Z for the trivalent actinides; $r_{42}$ is 0.84 for $U^{3+}$:$LaCl_3$ and 0.81 for $Pu^{3+}$:$LaCl_3$. This is the result of the actinide contraction and increased screening of the 5f electron as Z increases. For the borodeuterides we find that $r_{42}$ decreases from 0.97 to 0.93 in going from uranium to neptunium. Using the predicted value of 2253 $cm^{-1}$ for $\zeta_{\text{free ion}}$ of the $Np^{4+}$, we find that $k = \zeta/\zeta_{\text{free ion}}$ increases from 0.91 to 0.93. The predicted value of $F^2$ for the $Np^{4+}$ free ion leads to $\phi_2$ of .86 for $Np^{4+}$ vs. .81 for $U^{4+}$. These numbers are all consistent with increasing covalency with increasing oxidation number (as in the $nd^N$ series) and decreasing covalency with increasing Z for both the trivalent and tetravalent actinides. A crude model[18] where the actinide wave function is written as

$$\Psi = a\psi_{\text{metal}} + b\psi_{\text{ligand}}$$

predicts that, to a first approximation, the free-ion value of $\zeta$ is multiplied by $a^2$ and $F^2$ by $a^4$, i.e. $\phi_2 \simeq k^2$. Our results are consistent with such a model.

Since the matrix elements of $T^2$ are not linearly independent of those of the $F^k$'s, there is, in principle, a problem in comparing, as we have done above, calculations for $f^3$ (where $T^2$ is included) to those for $f^2$ where there is no $T^2$. Judd et al.[19,20] have suggested an alternate parameterization scheme, using orthogonalized operators, in which this problem does not arise. Table VII shows the Slater parameters and the new $\alpha'$, $\beta'$, and $\gamma'$ calculated from the results in Table V via the formulas of Ref. 20. Since $F^2$ is smaller

and $F^4$ relatively unchanged, the ratios $r_{42}$ are all slightly larger. There is a larger difference in the $\phi_2$ values for $U^{4+}$ and $Np^{4+}$ when the orthogonalized parameters are used. There are no differences in the trends, however; thus the conclusions drawn from the usual parameterization scheme remain unchanged.

From the wavefunctions and energies obtained from the optical analysis of $Np(BD_4)_4/Zr(BD_4)_4$, the reciprocal of the magnetic susceptibility vs. temperature and the ground $\Gamma_6$ state g value were calculated. Curve B in Fig. 5 shows the calculated reciprocal susceptibility. Table VIII gives the g values obtained for various values of the orbital reduction constant, k. With k = 0.862 the reciprocal magnetic susceptibility shown as curve C in Fig. 5 was obtained.

Without the introduction of the orbital reduction factor, the calculated g value for the ground state was too large. A lower value of k is needed to fit the methylborohydride g value, suggesting greater covalency in this molecule. Comparison of the k values for $U(BH_3CH_3)_4$ and $Np(BH_3CH_3)_4$ (Table VII) indicates somewhat less covalency for the neptunium compound. This is consistent with the optical results discussed above. In both the uranium and neptunium compounds the k from the optical analysis, which is an average over many levels, is larger than the k from the magnetic analysis which is sensitive only to the lower energy states.

It is noteworthy that the magnetic susceptibility of $Np(BH_3CH_3)_4$ could be fit within experimental error using the

energies and wavefunctions of the $Np(BD_4)_4/Zr(BD_4)_4$ analysis and adjusting only the orbital reduction factor. By contrast, the energy difference between the ground state and the first excited state also had to be adjusted in order to fit the $U(BH_3CH_3)_4$ data. However, for the Np compound there is a first order magnetic effect for the ground state which dominates the susceptibility while for the U compound the second order term is dominant because of the non-magnetic nature of the ground state.

Although a good fit to the magnetic data could be obtained by considering only the isolated $^4I_{9/2}$ term, the crystal field parameters and energy levels obtained are very different from those derived from the analysis of the optical data. One could be seriously misled by use of this oversimplified model if the criteria were only the agreement between the calculated susceptibility and g value and the experimental magnetic data.

## Conclusions

The energy levels of $Np(BD_4)_4/Zr(BD_4)_4$ have been analyzed with vibronic assignments and energy parameters which are consistent with those found for $U(BD_4)_4/Hf(BD_4)_4$. The least squares fit is worse, however; $\sigma$ is 84 $cm^{-1}$ for the neptunium crystal whereas it was 71 or 53 $cm^{-1}$ for uranium borodeuteride, depending on the choice of assignments. The free-ion parameters are not very well determined, but it is clear that a significant improvement in the fit will be possible only by modification of the crystal field Hamiltonian or

changes in many of the assignments.

If $\phi_2$, $r_{42}$ and k are used as measures of covalency, the parameter values indicate that covalency decreases with Z for the actinides and that the tetravalent actinides are more covalent than the trivalent actinides.

The magnetic data for $Np(BD_4)_4$ and $Np(BH_3CH_3)_4$ can be fit with the wavefunctions and energies obtained from the optical data only by the use of an orbital reduction factor. The values obtained for this parameter indicate that the methylborohydride compound is the more covalent.

Acknowledgments

We wish to thank John Conway for helpful discussions.

References

[a]This work was supported by the Director, Office of Energy Research, Office of Basic Energy Sciences, Chemical Sciences Division of the U.S. Department of Energy under Contract No. DE-AC03-76SF00098.

*Permanent address: Department of Physics, Kalamazoo College, Kalamazoo, Michigan 49007.

**Nalco Chemical Co., 1801 Diehl Road, Naperville, Il. 60540.

1. R. H. Banks, N. M. Edelstein, B. Spencer, D. H. Templeton, and A. Zalkin, J. Am. Chem. Soc. 102, 620 (1980).
2. K. Rajnak, E. Gamp, R. Shinomoto, and N. Edelstein, J. Chem. Phys. (preceding paper).
3. E. R. Bernstein and T. A. Keiderling, J. Chem. Phys. 59, 2105 (1973).
4. E. Gamp and N. Edelstein, J. Chem. Phys., following paper.
5. R. Shinomoto, E. Gamp, N. M. Edelstein, D. H. Templeton, and A. Zalkin, Inorg. Chem. (1983), in press.
6. G. Breit and I. Rabi, Phys. Rev. 38, 2002 (1931); see also: N. F. Ramsey, Molecular Beams, Oxford University Press, London, 1956, p. 86.
7. R. H. Banks and N. Edelstein, J. Chem. Phys. 73, 3589 (1980).

8. R. H. Banks and N. M. Edelstein in Lanthanide and Actinide Chemistry and Spectroscopy, N. Edelstein, Ed., ACS Symposium Series 131, Washington, D.C., 1980, p. 331.

9. W. T. Carnall, H. Crosswhite, H. M. Crosswhite, J. P. Hessler, N. M. Edelstein, J. G. Conway, G. V. Shalimoff, and R. Sarup, J. Chem. Phys. 72, 5089 (1980).

10. B. G. Wybourne, Spectroscopic Properties of Rare Earths, John Wiley and Sons, Inc., New York, 1965. Our definition for the crystal field parameters follows Wybourne's convention.

11. B. R. Judd, Phys. Rev. 141, 4 (1966).

12. R. D. Cowan and D. C. Griffin, J. Opt. Soc. Am. 66, 1010 (1976).

13. C. H. H. Van Deurzen, K. Rajnak, and J. G. Conway, J. Opt. Soc. Amer., 1983, submitted.

14. H. M. Crosswhite, H. Crosswhite, W. T. Carnall, and A. P. Paszek, J. Chem. Phys. 72, 5103 (1980).

15. K. Rajnak, E. Gamp, R. Banks, R. Shinomoto, and N. Edelstein, Inorg. Chim. Acta, to be published.

16. P. Delamoye, K. Rajnak, M. Genet, and N. Edelstein, Phys. Rev. B, in press.

17. D. C. Allen and K. D. Warren, Structure and Bonding 9, 49 (1971), 19, 105 (1974).

18. M. Gerloch and R. C. Slade, Ligand-Field Parameters, Cambridge Univ. Press, New York, 1973, p. 213.

19. B. R. Judd, Jorgen E. Hansen, and A. J. J. Raassen, J. Phys. B 15, 1457 (1982).

20. B. R. Judd and H. Crosswhite, J. Opt. Soc. B, to be published.

Table I. Spin Hamiltonian Parameters for $^{237}Np$ Borohydrides

| Host | $Zr(BH_3CH_3)_4$[a] | $CH_3C_6H_{11}$[b] | $Zr(BH_4)_4$[c] | $Zr(BD_4)_4$[d] |
|---|---|---|---|---|
| g | 1.7997(4)[e] | 1.8126(4) | 1.894(2) | 1.891(2) |
| A ($cm^{-1}$) | 0.1122(2) | 0.1124(1) | 0.1140(10) | 0.1140(10) |

[a] $^{237}Np(BH_3CH_3)_4/Zr(BH_3CH_3)_4$.
[b] frozen solution (glass).
[c] $^{237}Np(BH_4)_4/Zr(BH_4)_4$.
[d] $^{237}Np(BD_4)_4/Zr(BD_4)_4$.
[e] averaged ("isotropic") values.

Table II. Absorption spectrum of $Np(BD_4)_4/Zr(BD_4)_4$ at 2 K: summary of electronic and vibrational assignments

| λ(nm) | Estimated Uncertainty (± nm) | Relative Intensity | Vacuum Corrected Energy ($cm^{-1}$) | Assignment to Origins + Δν ($cm^{-1}$) | Vibrational Identification |
|---|---|---|---|---|---|
| 1783.8 | 0.15 | 42 | 5605 | origin a | |
| 1770.0 | 0.5 | 4 | 5648 | a + 43 | xx |
| 1746.1 | 0.2 | 24 | 5726 | a + 121 | a + β |
| 1740.9 | 0.2 | 17 | 5743 | a + 138 | xxx |
| 1735.4 | 0.2 | 17 | 5761 | a + 156 | a + δ |
| 1730.6 | 0.2 | 29 | 5777 | a + 172 | a + ε |
| 1710.4 | 0.3 | 3 | 5845 | a + 240 | a + 2β |
| 1705.3 | 0.3 | 2 | 5863 | a + 258 | a + β + xxx |
| 1700.6 | 1.0 | 1.5 | 5879 | a + 274 | a + β + δ |
| 1695.7 | 0.3 | 5 | 5896 | a + 291 | a + β + ε |
| 1690.2 | 0.5 | 1.5 | 5915 | a + 310 | a + 2δ |
| 1680.0 | 1.0 | 0.5 | 5951 | a + 346 | a + 2ε |
| 1670.0 | 0.6 | 1 | 5986 | a + 381 | a + 2β + xxx |
| 1662.4 | 1.0 | 0.4 | 6014 | a + 409 | a + ζ |
| 1656.5 | 0.3 | 4 | 6035 | a + 430 | a + η' |
| 1650.6 | 0.2 | 22 | 6057 | a + 452 | a + η |
| 1644.6 | 0.2 | 10 | 6079 | a + 474 | a + θ |
| 1624.6 | 0.5 | 1 | 6154 | a + 549 | a + η' + β |
| 1618.3 | 0.4 | 3 | 6177 | a + 572 | a + η + β |
| 1613.5 | 0.9 | 2 | 6196 | a + 591 | a + xxx + η |
| 1562.6 | 0.3 | 4 | 6398 | a + 793 | a + χ |
| 1560.1 | 0.2 | 9 | 6408 | a + 803 | a + κ |
| 1550.9 | 0.3 | 2 | 6446 | a + 841 | a + ζ + η' |
| 1545.0 | 0.2 | 7 | 6471 | a + 866 | a + Ξ |

Table II. Continued

| λ(nm) | Estimated Uncertainty (± nm) | Relative Intensity | Vacuum Corrected Energy ($cm^{-1}$) | Assignment to Origins + Δν ($cm^{-1}$) | Vibrational Identification |
|---|---|---|---|---|---|
| 1533.5 | 1.5 | 3 | 6519 | a + 914 | a + λ |
| 1530.0 | 1.0 | 4 | 6534 | a + 929 | a + λ' |
| 1516.6 | 0.6 | 1 | 6592 | a + 987 | a + 2η' + β |
| 1411.4 | 0.1 | 98 | 7083 | origin b | |
| 1403.9 | 0.2 | 19 | 7121 | a + 1516 | a + ξ |
| | | | | b + 38 | b + xx |
| 1400.9 | 0.3 | 21 | 7136 | a + 1531 | a + ξ' |
| 1398.8 | 0.6 | 19 | 7147 | a + 1542 | a + ξ" |
| 1388.2 | 0.4 | 15 | 7202 | b + 119 | b + β |
| 1378.8 | 0.3 | 35 | 7251 | b + 168 | b + δ |
| | | | | a + 1646 | a + ξ' + β |
| 1375.5 | 0.25 | 37 | 7268 | b + 185 | b + ε |
| | | | | a + 1663 | a + ξ" + β |
| 1367.5 | 1.5 | 15 | 7311 | a + 1706 | a + ξ' + ε |
| 1354.5 | 1.0 | 12 | 7381 | b + 298 | b + β + ε |
| | | | | a + 1776 | a + ξ" + 2β |
| 1348.2 | 1.0 | 9 | 7415 | b + 368 | b + 2ε |
| 1333.3 | 0.5 | 8 | 7498 | b + 415 | b + ζ |
| 1325.6 | 0.2 | 32 | 7542 | b + 459 | b + η |
| 1316.5 | 0.3 | 28 | 7594 | origin c | |
| | | | | b + 511 | b + 3δ |
| 1313.2 | 0.3 | 25 | 7613 | b + 530 | b + 2ε + δ |
| | | | | | b + β + ζ |
| 1300.0 | 2.0 | ~ 230 | 7690 | c + 96 | c + β |
| | | | | b + 607 | b + δ + η |
| | | | | | b + ζ + ε |
| 1273.5 | 0.6 | 20 | 7850 | c + 256 | c + β + δ |
| 1267.4 | 0.5 | 16 | 7887 | c + 294 | c + 3β |

Table II Continued

| λ(nm) | Estimated Uncertainty (± nm) | Relative Intensity | Vacuum Corrected Energy ($cm^{-1}$) | Assignment to Origins + Δν ($cm^{-1}$) | Vibrational Identification |
|---|---|---|---|---|---|
| 1263.9 | 1.0 | 15 | 7910 | c + 316 | c + 2δ |
| | | | | b + 827 | b + κ |
| 1260.9 | 0.5 | 14 | 7929 | b + 846 | b + Ξ |
| 1248.8 | 0.3 | 13 | 8006 | b + 923 | b + λ' |
| | | | | c + 412 | c + ζ |
| 1241.8 | 0.5 | 12 | 8051 | c + 457 | c + η |
| 1225.8 | 1.0 | 25 | 8156 | c + 562 | c + η + β |
| | | | | b + 1073 | b + Ξ + 2β |
| 1178.0 | 0.6 | 7 | 8487 | c + 893 | c + λ |
| 1173.0 | 0.9 | 5 | 8523 | c + 929 | c + λ' |
| 1162.4 | 0.5 | 6 | 8601 | b + 1518 | b + ξ |
| | | | | c + 1037 | c + λ' + β |
| 1158.3 | 1.2 | 7 | 8631 | b + 1548 | b + ξ" |
| | | | | a + 3026 | a + 2ξ |
| 1152.4 | 1.2 | 5 | 8675 | c + 1081 | c + λ' + δ |
| | | | | a + 3070 | a + 2ξ' |
| 1128.2 | 1.7 | 3 | 8861 | b + 1778 | b + Ξ + λ' |
| | | | | c + 1267 | c + λ' + 2δ |
| 1077.2 | 0.4 | 5 | 9281 | origin d | |
| 1071.2 | 1.5 | 3 | 9333 | d + 52 | d + xx |
| 1063.2 | 0.2 | 19 | 9403 | d + 122 | d + β |
| 1058.0 | 0.15 | 45 | 9449 | d + 168 | d + δ |
| 1050.2 | 0.2 | 4 | 9519 | d + 238 | d + 2β |
| 1044.5 | 0.2 | 15 | 9571 | origin e | |
| | | | | d + 290 | d + β + δ |
| 1040.0 | 0.7 | 3 | 9613 | d + 332 | d + 2δ |
| | | | | e + 48 | e + xx |
| 1030.0 | 1.3 | 12 | 9706 | d + 425 | d + η' |

Table II Continued

| λ(nm) | Estimated Uncertainty (± nm) | Relative Intensity | Vacuum Corrected Energy ($cm^{-1}$) | Assignment to Origins + Δν ($cm^{-1}$) | Vibrational Identification |
|---|---|---|---|---|---|
| 1026.8 | 0.2 | 20 | 9736 | d + 455 | d + η |
| | | | | e + 165 | e + δ |
| 1014.0 | 0.5 | 3 | 9859 | d + 578 | d + β + η |
| | | | | e + 288 | e + β + δ |
| 1001.3 | 0.3 | 6 | 9984 | d + 703 | d + η + 2β |
| | | | | e + 413 | e + ζ |
| 997.0 | 0.2 | 13 | 10027 | e + 456 | e + η |
| 991.8 | 0.2 | 12 | 10080 | d + 799 | d + χ |
| 985.2 | 0.2 | 9 | 10147 | d + 866 | d + Ξ |
| 980.0 | 0.5 | 10 | 10201 | d + 920 | d + λ |
| 967.3 | 0.15 | 80 | 10335 | d + 1054 | d + λ + β |
| | | | | e + 764 | e + χ |
| 953.5 | 0.2 | 19 | 10485 | e + 914 | e + λ(2η) |
| 945.3 | 0.3 | 27 | 10576 | d + 1295 | d + λ + 3β |
| | | | | e + 1005 | e + χ + 2β |
| 933.5 | 1.2 | 9 | 10709 | origin f | |
| | | | | d + 1428 | d + δ + η + χ |
| | | | | e + 1138 | e + λ + 2β |
| 926.0 | 0.2 | 8 | 10796 | d + 1515 | d + ξ |
| 918.8 | 1.5 | 4 | 10881 | f + 172 | f + ε |
| 898.9 | 0.3 | 7 | 11122 | f + 413 | f + ζ |
| 894.7 | 0.9 | 4 | 11174 | f + 465 | f + θ |
| 866.7 | 1.0 | ~ 180 | 11535 | origin g | |
| | | | | f + 826 | f + κ(2ζ) |
| 855.7 | 0.8 | 50 | 11683 | g + 148 | g + δ |
| 845.7 | 1.3 | 7 | 11821 | g + 286 | g + 2δ |
| 834.6 | 0.2 | 62 | 11978 | g + 443 | g + η |

Table II Continued

| λ(nm) | Estimated Uncertainty (± nm) | Relative Intensity | Vacuum Corrected Energy ($cm^{-1}$) | Assignment to Origins + Δν ($cm^{-1}$) | Vibrational Identification |
|---|---|---|---|---|---|
| 821.5 | 0.1 | 165 | 12170 | origin h | |
| 807.0 | 5.0 | > 400 | 12388 | h + 218 | g + 2β |
| | | | | g + 853 | g + Ξ |
| 792.0 | ~ 2.5 | ~ 55 | 12623 | origin i | |
| | | | | h + 453 | h + η |
| 780.0 | ~ 4.0 | ~ 30 | 12817 | i + 194 | i + ε |
| | | | | h + 647 | h + η + ε |
| 771.2 | 1.0 | 93 | 12963 | origin j | |
| | | | | h + 793 | h + χ |
| 768.7 | 0.2 | 101 | 13005 | j + 42 | j + xx |
| | | | | h + 835 | h + κ |
| | | | | i + 383 | i + 2ε |
| 764.1 | 1.0 | 78 | 13084 | h + 914 | h + λ |
| | | | | j + 121 | j + β |
| | | | | i + 461 | i + η |
| 745.2 | 1.0 | 22 | 13416 | origin k | |
| | | | | j + 453 | j + η |
| 738.9 | 0.2 | 37 | 13530 | k + 114 | k + β |
| | | | | j + 567 | j + β + η |
| 725.6 | 0.2 | 100 | 13778 | origin ℓ | |
| | | | | k + 248 | k + 2β |
| 718.8 | 0.7 | 66 | 13908 | ℓ + 130 | ℓ + β |
| 713.8 | 0.2 | 66 | 14006 | origin m | |
| 706.1 | 0.5 | 43 | 14158 | m + 152 | m + δ |
| 695.7 | 0.4 | 38 | 14370 | origin n | |
| 692.4 | 1.4 | 32 | 14439 | origin o | |
| 685.5 | 1.2 | 26 | 14584 | o + 145 | o + δ |
| | | | | ℓ + 806 | ℓ + κ |

Table II Continued

| λ(nm) | Estimated Uncertainty (± nm) | Relative Intensity | Vacuum Corrected Energy ($cm^{-1}$) | Assignment to Origins + Δν ($cm^{-1}$) | Vibrational Identification |
|---|---|---|---|---|---|
| 675.9 | 0.6 | 32 | 14791 | origin p | |
| 670.6 | 0.3 | 23 | 14908 | p + 117 | p + β |
| 664.7 | 1.5 | 15 | 15040 | p + 249 | p + 2β |
| | | | | o + 601 | o + δ + η |
| 654.7 | 0.5 | 17 | 15270 | origin q | |
| | | | | ℓ + 1493 | ℓ + ξ |
| | | | | p + 479 | p + θ |
| | | | | o + 831 | o + κ |
| 650.5 | 2.0 | 14 | 15369 | q + 99 | q + β |
| | | | | o + 930 | o + λ' |
| 642.4 | 0.4 | 9 | 15562 | q + 292 | q + 3β |
| | | | | p + 771 | p + χ |
| 635.9 | 1.2 | 8 | 15721 | q + 451 | q + η |
| | | | | p + 930 | p + λ' |
| 629.2 | 0.7 | 6 | 15889 | origin r | |
| | | | | p + 1098 | p + λ' + δ |
| | | | | q + 619 | q + η + δ |
| 616.2 | 0.3 | 7 | 16224 | origin s | |
| | | | | q + 954 | q + λ' |
| 613.2 | 0.3 | 11 | 16303 | p + 1512 | p + ξ |
| | | | | r + 414 | r + ζ |
| 602.2 | 0.2 | 46 | 16601 | origin t | |
| 584.1 | 1.0 | 11 | 17116 | origin u | |
| 583.0 | 0.8 | 11 | 17148 | s + 924 | s + λ' |
| 570.0 | 2.0 | 4 | 17539 | u + 423 | u + η' |
| | | | | t + 938 | t + λ' |
| 563.5 | 1.0 | 2 | 17741 | s + 1517 | s + ξ |
| 555.3 | 0.5 | 4 | 18003 | u + 887 | u + Ξ |

Table II Continued

| λ(nm) | Estimated Uncertainty (± nm) | Relative Intensity | Vacuum Corrected Energy ($cm^{-1}$) | Assignment to Origins + Δν ($cm^{-1}$) | Vibrational Identification |
|---|---|---|---|---|---|
| | | | | t + 1402 | t + λ' + θ |
| 552.4 | 1.0 | 4 | 18098 | t + 1497 | t + ξ |
| 543.2 | 0.4 | 9 | 18404 | origin v | |
| 540.1 | 0.3 | 10 | 18510 | v + 106 | v + β |
| 530.1 | 0.6 | 7 | 18859 | origin w | |
| 521.8 | 0.7 | 9 | 19159 | origin x | |
| 519.5 | 0.4 | 12 | 19244 | origin y | |
| 517.6 | 1.0 | 9 | 19315 | x + 156 | x + δ |
| ~510.0 | 2.0 | 8 | 19602 | x + 443 | x + η |
| 503.5 | 0.2 | 30 | 19855 | origin z | |
| 501.2 | 1.5 | 15 | 19947 | y + 92 | y + β |
| 495.5 | 0.2 | 32 | 20176 | origin aa | |
| 491.4 | 0.3 | 22 | 20344 | origin bb | |
| 484.5 | 0.3 | 18 | 20634 | origin cc | |
| 481.2 | 1.2 | 15 | 20776 | origin dd | |
| 474.7 | 1.2 | 60 | 21060 | origin ee | |
| 472.1 | 0.4 | 76 | 21176 | ee + 116 | ee + β |
| 461.3 | 0.8 | 14 | 21672 | aa + 1496 | aa + ξ |
| 455.4 | 0.5 | 12 | 21953 | origin ff | |
| | | | | ee + 893 | ee + λ |
| 450.0 | 0.3 | 14 | 22216 | origin gg | |
| 448.3 | 1.5 | 11 | 22300 | cc + 1524 | cc + ξ' |
| 439.1 | 0.2 | 24 | 22767 | origin hh | |
| 429.3 | 0.2 | 15 | 23287 | origin ii | |
| 427.1 | 1.5 | 9 | 23407 | origin jj | |
| | | | | ii + 120 | ii + β |

Table II Continued

| λ(nm) | Estimated Uncertainty (± nm) | Relative Intensity | Vacuum Corrected Energy ($cm^{-1}$) | Assignment to Origins + Δν ($cm^{-1}$) | Vibrational Identification |
|---|---|---|---|---|---|
| 421.8 | 0.5 | 7 | 23701 | ii + 414 | ii + ζ |
| | | | | hh + 934 | hh + λ' |
| 414.1 | 1.5 | 5 | 24142 | ii + 855 | ii + Ξ |
| 411.3 | 0.5 | 7 | 24306 | origin kk | |
| 403.9 | 0.7 | 8 | 24752 | origin ℓℓ | |
| 402.5 | 1.0 | 8 | 24838 | ii + 1551 | ii + ξ" |
| 397.9 | 0.2 | 13 | 25125 | origin mm | |
| 396.5 | 1.5 | 10 | 25214 | mm + 89 | mm + β |
| 393.5 | 1.0 | 13 | 25406 | origin nn | |
| 390.2 | 0.2 | 23 | 25621 | mm + 496 | mm + θ |
| | | | | ℓℓ + 869 | ℓℓ + Ξ |
| 385.9 | 0.2 | 25 | 25906 | origin oo | |
| ~380.0 | 7.5 | ~ 10 | 26308 | oo + 402 | oo + ζ |
| 369.2 | 2.0 | ~ 4 | 27078 | origin pp | |
| 367.1 | 1.5 | ~ 4 | 27233 | origin qq | |
| 360.0 | 0.2 | 9 | 27770 | origin rr | |
| 355.3 | 0.3 | 12 | 28137 | origin ss | |

Table III. Vibrational energies associated with $Np(BD_4)_4/Zr(Bd_4)_4$ origins

| Origin | xx | β | δ | ε | ζ | η' | η | θ | χ | κ | Ξ | λ | λ' | ξ | ξ' | ξ'' |
|---|---|---|---|---|---|---|---|---|---|---|---|---|---|---|---|---|
| a | 43 | 121 | 156 | 172 | 409 | 430 | 452 | 474 | 793 | 803 | 866 | 914 | 929 | 1516 | 1531 | 1542 |
| b | 38 | 119 | 168 | 185 | 415 | – | 459 | – | 805 | 827 | 846 | – | 923 | 1518 | – | 1548 |
| c | – | 96 | 160 | – | 412 | – | 457 | – | – | – | – | 893 | 929 | – | – | – |
| d | 52 | 122 | 168 | – | – | 425 | 455 | – | 799 | – | 866 | 920 | – | 1515 | – | – |
| e | 48 | 123 | 165 | – | 413 | – | 456 | – | 764 | – | – | 914 | – | – | – | – |
| f | – | – | – | 172 | 413 | – | – | 465 | – | 826 | – | – | – | – | – | – |
| g | – | – | 148 | – | – | – | 443 | – | – | – | 853 | – | – | – | – | – |
| h | – | 109 | – | – | – | – | 453 | – | 793 | 835 | – | 914 | – | – | – | – |
| i | – | – | 146 | 194 | – | – | 461 | – | 761 | – | – | – | – | – | – | – |
| j | 42 | 121 | – | – | – | – | 453 | – | – | – | – | – | – | – | – | – |
| k | – | 114 | – | – | – | – | – | – | – | – | – | – | – | – | – | – |
| ℓ | – | 130 | – | – | – | – | – | – | – | 806 | – | – | – | 1493 | – | – |
| m | – | – | 152 | – | – | – | 456 | – | – | – | – | – | – | – | – | – |
| n | – | – | – | – | – | – | – | – | – | – | – | – | – | – | – | – |
| o | – | – | 145 | – | – | – | 456 | – | – | 831 | – | – | 930 | – | – | – |
| p | – | 117 | – | – | – | – | – | 479 | 771 | – | – | – | 930 | 1512 | – | – |
| q | – | 99 | 168 | – | – | – | 451 | – | – | – | – | – | 954 | – | – | – |
| r | – | – | – | – | 414 | – | – | – | – | – | – | – | – | – | – | – |
| s | – | – | – | – | – | – | – | – | – | – | – | – | 924 | 1517 | – | – |
| t | – | – | – | – | – | – | – | 464 | – | – | – | – | 938 | 1497 | – | – |
| u | – | – | – | – | – | 423 | – | – | – | – | 887 | – | – | – | – | – |
| v | – | 106 | – | – | – | – | – | – | – | – | – | – | – | – | – | – |
| w | – | – | – | – | – | – | – | – | – | – | – | – | – | – | – | – |
| x | – | – | 156 | – | – | – | 443 | – | – | – | – | – | – | – | – | – |
| y | – | 92 | – | – | – | – | – | – | – | – | – | – | – | – | – | – |
| z | – | – | – | – | – | – | – | – | – | – | – | – | – | – | – | – |
| aa | – | – | – | – | – | – | – | – | – | – | – | – | – | 1496 | – | – |
| bb | – | – | – | – | – | – | – | – | – | – | – | – | – | – | – | – |
| cc | – | – | – | – | – | – | – | – | – | – | – | – | – | – | 1524 | – |
| dd | – | – | – | – | – | – | – | – | – | – | – | – | – | – | – | – |

Table III. Continued

| Origin | xx | β | δ | ε | ζ | η' | η | θ | χ | κ | Ξ | λ | λ' | ξ | ξ' | ξ" |
|---|---|---|---|---|---|---|---|---|---|---|---|---|---|---|---|---|
| ee | – | 116 | – | – | – | – | – | – | – | – | – | 893 | – | – | – | – |
| ff | – | – | – | – | – | – | – | – | – | – | – | – | – | – | – | – |
| gg | – | – | – | – | – | – | – | – | – | – | – | – | – | – | – | – |
| hh | – | – | – | – | – | – | – | – | – | – | – | – | 934 | – | – | – |
| ii | – | 120 | – | – | 414 | – | – | – | – | – | 855 | – | – | – | – | 1551 |
| jj | – | – | – | – | – | – | – | – | – | – | – | – | – | – | – | – |
| kk | – | – | – | – | – | – | – | – | – | – | – | – | – | – | – | – |
| ℓℓ | – | – | – | – | – | – | – | – | – | – | 869 | – | – | – | – | – |
| mm | – | 89 | – | – | – | – | – | 496 | – | – | – | – | – | – | – | – |
| nn | – | – | – | – | – | – | – | – | – | – | – | – | – | – | – | – |
| oo | – | – | – | – | 402 | – | – | – | – | – | – | – | – | – | – | – |
| pp | – | – | – | – | – | – | – | – | – | – | – | – | – | – | – | – |
| qq | – | – | – | – | – | – | – | – | – | – | – | – | – | – | – | – |
| rr | – | – | – | – | – | – | – | – | – | – | – | – | – | – | – | – |

Table IV. HFR parameters ($cm^{-1}$) for $U^{4+}$ and $Np^{4+}$

| | $U^{4+}$ | $Np^{4+}$ |
|---|---|---|
| $F^2$ | 76652 | 79831 |
| $F^4$ | 50147 | 52279 |
| $F^6$ | 36828 | 38413 |
| $\zeta$ | 2092 | 2377 |
| $M^0$ | 0.773 | 0.876 |
| $M^2$ | 0.430 | 0.487 |
| $M^4$ | 0.299 | 0.339 |

Table V. Parameter values ($cm^{-1}$) for trivalent and tetravalent Np and U[a]

| | $Np(BD_4)_4$/ $Zr(BD_4)_4$ | $U(BD_4)_4$/ $Hf(BD_4)_4$[b] | $U^{3+}:LaCl_3$[c] | $Np^{3+}:LaCl_3$[c] |
|---|---|---|---|---|
| $F^2$ | 46689(415) | 41280(175) | 39715(218) | 44907(161) |
| $F^4$ | 43239(645) | 40013(826) | 33537(302) | 36918(245) |
| $F^6$ | 26303(722) | 22554(625) | 23670(211) | 25766(221) |
| $\zeta$ | 2089(10) | 1782(12) | 1623(4) | 1938(2) |
| $\alpha$ | 40(2) | 38(2) | 27.6(0.9) | 31.5(0.3) |
| $\beta$ | [-600] | [-648] | -722(33) | -740(18) |
| $\gamma$ | [1200] | [1200] | [1000] | 899(70) |
| $M^0$ | [0.88] | [0.987] | [0.67] | 0.68(0.17) |
| $M^2$ | [0.49] | [0.550] | d | d |
| $M^4$ | [0.34] | [0.384] | d | d |
| $P^2$ | [500] | [500] | 1276(104)[e] | 894(14)[e] |
| $P^4$ | [500] | [500] | - | - |
| $P^6$ | [500] | [500] | - | - |
| $T^2$ | [278] | - | 217(90) | 278(22) |
| $T^3$ | [44] | - | 63(13) | 44(7) |
| $T^4$ | [64] | - | 255(23) | 64(7) |
| $T^6$ | [-361] | - | -107(49) | -361(18) |
| $T^7$ | [434] | - | 617(78) | 434(22) |
| $T^8$ | [353] | - | [350] | 353(17) |
| $B_0^4$ | -2722(182) | -2445(124) | -532(139) | -632(48) |
| $B_0^6$ | -5070(69) | -5371(81) | -1438(113) | -1625(52) |

Table V continued.

| | $Np(BD_4)_4$/ $Zr(BD_4)_4$ | $U(BD_4)_4$/ $Hf(BD_4)_4$[b] | $U^{3+}:LaCl_3$[c] | $Np^{3+}:LaCl_3$[c] |
|---|---|---|---|---|
| $\sigma$ | 84 | 53 | 26 | 20 |
| k | 0.93[f] | 0.91 | - | - |
| $\phi_2$ | 0.86[f] | 0.81 | - | - |
| $r_{42}$ | 0.93 | 0.97 | 0.84 | 0.82 |

a rms errors are in ( ). Values in [ ] were held fixed.
b Ref. 2.
c Ref. 14.
d $M^2$ and $M^4$ constrained to vary as $M^2/M^0 = 0.56$, $M^4/M^0 = 0.38$.
e $P^4$ and $P^6$ constrained to vary as $P^4/P^2 = 0.75$, $P^6/P^2 = 0.50$.
f. Based on estimated free-ion parameters $\zeta = 2253$ and $F^2 = 54463$ $cm^{-1}$.

Table VI. Observed and calculated energy levels ($cm^{-1}$) of $Np(BD_4)_4/Zr(BD_4)_4$

| Γ | $E_{calc}$ | $E_{obs}$ | $\Delta E$[a] | Eigenvector[b] |
|---|---|---|---|---|
| 6 | 0 | 0 | 0 | $82\ ^4I_{9/2} + 10\ ^2H2_{9/2}$ |
| 8 | 457 | – | – | $75\ ^4I_{9/2} + 10\ ^2H2_{9/2}$ |
| 8 | 2205 | – | – | $68\ ^4I_{9/2} + 17\ ^2H2_{9/2}$ |
| 8 | 5620 | 5605 | 15 | $67\ ^4I_{11/2} + 10\ ^4F_{3/2}$ |
| 6 | 7193 | – | – | $86\ ^4I_{11/2} + 3\ ^2H2_{11/2}$ |
| 8 | 7193 | 7083 | 110 | $66\ ^4I_{11/2} + 9\ ^4I_{9/2}$ |
| 7 | 7490 | 7594 | 104 | $85\ ^4I_{11/2} + 6\ ^4I_{13/2}$ |
| 8 | 9387 | 9281 | 106 | $39\ ^4F_3 + 16\ ^2D1_{3/2}$ |
| 7 | 9596 | 9571 | 25 | $49\ ^4I_{13/2} + 16\ ^4F_{5/2}$ |
| 8 | 10777 | 10709 | 68 | $45\ ^4I_{13/2} + 9\ ^4I_{15/2}$ |
| 6 | 11575 | – | – | $81\ ^4I_{13/2} + 5\ ^4I_{15/2}$ |
| 8 | 11579 | 11535 | 44 | $38\ ^4I_{13/2} + 14\ ^4F_{5/2}$ |
| 7 | 12277 | 12170 | 108 | $64\ ^4I_{13/2} + 9\ ^4F_{7/2}$ |
| 8 | 12598 | 12623 | -25 | $18\ ^2H2_{9/2} + 16\ ^4I_{9/2}$ |
| 8 | 13003 | 12963 | 40 | $21\ ^2H2_{9/2} + 11\ ^2G1_{9/2}$ |
| 8 | 13327 | 13416 | -89 | $19\ ^4I_{13/2} + 15\ ^4F_{5/2}$ |
| 6 | 13614 | – | – | $30\ ^2H2_{9/2} + 11\ ^4F_{7/2}$ |
| 8 | 13741 | 13778 | -37 | $29\ ^4G_{5/2} + 26\ ^4I_{15/2}$ |
| 7 | 13929 | 14006 | -77 | $43\ ^4I_{15/2} + 30\ ^4I_{13/2}$ |
| 7 | 14297 | 14370 | -73 | $27\ ^4I_{13/2} + 25\ ^4G_{5/2}$ |
| 8 | 14375 | 14439 | -64 | $18\ ^4I_{15/2} + 17\ ^4G_{5/2}$ |

Table VI continued.

| Γ | $E_{calc}$ | $E_{obs}$ | $\Delta E$[a] | Eigenvector[b] |
|---|---|---|---|---|
| 6 | 14584 | - | - | 44 $^4F_{7/2}$ + 15 $^2Gl_{7/2}$ |
| 7 | 14736 | 14791 | -55 | 40 $^4F_{5/2}$ + 28 $^4G_{5/2}$ |
| 8 | 15279 | 15270 | 9 | 31 $^4F_{7/2}$ + 17 $^2Gl_{7/2}$ |
| 7 | 15945 | 15889 | -56 | 27 $^4F_{7/2}$ + 20 $^2Gl_{7/2}$ |
| 8 | 16149 | 16224 | -75 | 30 $^4I_{15/2}$ + 14 $^4S_{3/2}$ |
| 6 | 16549 | - | - | 42 $^4I_{15/2}$ + 15 $^2K_{15/2}$ |
| 8 | 16628 | 16601 | 27 | 33 $^4G_{7/2}$ + 24 $^4I_{15/2}$ |
| 8 | 17074 | 17116 | -42 | 54 $^4I_{15/2}$ + 11 $^2K_{15/2}$ |
| 6 | 17682 | - | - | 41 $^4G_{7/2}$ + 17 $^4F_{7/2}$ |
| 7 | 18552 | 18404 | 148 | 51 $^4G_{7/2}$ + 22 $^4F_{7/2}$ |
| 8 | 18814 | 18859 | -45 | 18 $^4G_{7/2}$ + 9 $^4F_{9/2}$ |
| 8 | 19048 | 19159 | -111 | 21 $^2H2_{11/2}$ 8 $^4G_{7/2}$ |
| 6 | 19221 | - | - | 21 $^2P_{1/2}$ + 15 $^4D_{1/2}$ |
| 8 | 19234 | 19244 | -10 | 16 $^2H2_{11/2}$ + 11 $^4G_{11/2}$ |
| 8 | 19706 | 19885 | - | 32 $^4K_{13/2}$ + 28 $^4F_{9/2}$ |
| 6 | 19725 | - | - | 21 $^4G_{7/2}$ + 20 $^4F_{9/2}$ |
| 7 | 20190 | 20176 | 14 | 49 $^2K_{13/2}$ + 9 $^4I_{13/2}$ |
| 8 | 20324 | 20344 | -20 | 26 $^4F_{9/2}$ + 11 $^4I_{15/2}$ |
| 8 | 20668 | 20634 | 34 | 12 $^2H2_{11/2}$ + 11 $^4G_{9/2}$ |
| 7 | 20684 | 20776 | -92 | 29 $^2H2_{11/2}$ + 15 $^2K_{13/2}$ |
| 6 | 21008 | - | - | 27 $^2K_{13/2}$ + 16 $^2G_{9/2}$ |

Table VI continued.

| $\Gamma$ | $E_{calc}$ | $E_{obs}$ | $\Delta E$[a] | Eigenvector[b] |
|---|---|---|---|---|
| 8 | 21110 | 21060 | 50 | $46\ {}^4G_{9/2} + 10\ {}^4D_{5/2}$ |
| 8 | 21453 | – | – | $20\ {}^2H2_{11/2} + 15\ {}^2K_{13/2}$ |
| 6 | 21831 | – | – | $25\ {}^2G1_{7/2} + 19\ {}^2G2_{7/2}$ |
| 8 | 22092 | 21953 | 139 | $23\ {}^2K_{13/2} + 13\ {}^4F_{7/2}$ |
| 7 | 22220 | 22216 | 4 | $66\ {}^2K_{13/2} + 6\ {}^4D_{5/2}$ |
| 7 | 22526 | – | – | $24\ {}^2G1_{7/2} + 15\ {}^4F_{7/2}$ |
| 8 | 22561 | – | – | $29\ {}^4G_{9/2} + 12\ {}^2H2_{11/2}$ |
| 6 | 22576 | – | – | $27\ {}^4D_{1/2} + 17\ {}^2P_{1/2}$ |
| 7 | 22643 | 22767 | -124 | $18\ {}^4D_{5/2} + 18\ {}^2H2_{11/2}$ |
| 8 | 22230 | 23287 | -57 | $36\ {}^2K_{13/2} + 17\ {}^4G_{9/2}$ |
| 6 | 23419 | – | – | $24\ {}^4G_{9/2} + 17\ {}^2K_{13/2}$ |
| 8 | 23421 | 23407 | 14 | $12\ {}^2L_{15/2} + 10\ {}^4G_{9/2}$ |
| 8 | 24291 | 24306 | -15 | $19\ {}^4D_{5/2} + 13\ {}^2K_{15/2}$ |
| 7 | 24443 | – | – | $38\ {}^2K_{15/2} + 24\ {}^2L_{15/2}$ |
| 6 | 24621 | – | – | $19\ {}^2K_{15/2} + 14\ {}^2L_{15/2}$ |
| 8 | 24641 | 24752 | -111 | $27\ {}^4D_{3/2} + 7\ {}^4G_{9/2}$ |
| 8 | 25223 | 25125 | 98 | $15\ {}^2L_{15/2} + 11\ {}^2K_{15/2}$ |
| 8 | 25399 | 25406 | -7 | $17\ {}^2H1_{11/2} + 19\ {}^2L_{15/2}$ |
| 8 | 25897 | 25906 | – | $19\ {}^4G_{11/2} + 18\ {}^2D1_{5/2}$ |
| 7 | 25976 | – | – | $32\ {}^2H1_{11/2} + 24\ {}^2I_{11/2}$ |
| 8 | 26137 | – | – | $24\ {}^2H1_{11/2} + 19\ {}^4G_{11/2}$ |

Table VI continued.

| Γ | $E_{calc}$ | $E_{obs}$ | $\Delta E$[a] | Eigenvector[b] |
|---|---|---|---|---|
| 6 | 26277 | - | - | $28\ ^2L_{15/2} + 13\ ^2Hl_{11/2}$ |
| 8 | 26595 | - | - | $19\ ^2D_{5/2} + 16\ ^2L_{15/2}$ |
| 8 | 26864 | - | - | $12\ ^2P_{3/2} + 11\ ^2Gl_{9/2}$ |
| 8 | 27167 | 27078 | 89 | $24\ ^2I_{11/2} + 19\ ^2Hl_{11/2}$ |
| 7 | 27243 | 27233 | 10 | $53\ ^2Dl_{5/2} + 16\ ^2Hl_{11/2}$ |
| 6 | 27702 | 27698 | - | $17\ ^2I_{11/2} + 16\ ^2Gl_{9/2}$ |
| 8 | 27949 | 27770 | 179 | $31\ ^4G_{11/2} + 15\ ^2I_{11/2}$ |
| 7 | 28120 | 28137 | 17 | $34\ ^4G_{11/2} + 29\ ^2I_{15/2}$ |
| 8 | 28741 | - | - | $14\ ^2D2_{3/2} + 9\ ^2I_{13/2}$ |
| 6 | 28835 | - | - | $27\ ^2P_{1/2} + 17\ ^2Hl_{11/2}$ |
| 6 | 29021 | - | - | $24\ ^4D_{9/2} + 15\ ^2I_{11/2}$ |
| 8 | 29379 | - | - | $70\ ^4D_{7/2} + 4\ ^2Fl_{7/2}$ |
| 6 | 29699 | - | - | $38\ ^4D_{7/2} + 20\ ^4G_{11/2}$ |
| 7 | 29715 | - | - | $79\ ^4D_{7/2} + 5\ ^2Fl_{7/2}$ |

[a] $\Delta E = E_{calc} - E_{obs}$

[b] percentage of SLJ state, 2 largest components

Table VII. Parameter values ($cm^{-1}$) associated with the orthogonalized operators of Judd and Crosswhite[a]

| | $Np(BD_4)_4$/ $Zr(BD_4)_4$ | $U(BD_4)_4$/ $Hf(BD_4)_4$[b] | $U^{3+}$:$LaCl_3$[c] | $Np^{3+}$:$LaCl_3$[c] |
|---|---|---|---|---|
| $F^2$ | 46068 | 40689 | 39268 | 44360 |
| $F^4$ | 43182 | 39956 | 33450 | 36721 |
| $F^6$ | 29044 | 25154 | 25507 | 27753 |
| $\alpha'$ | 32.0 | 30.4 | 22 | 25.2 |
| $\beta'$ | -60 | -44 | 9.9 | -2.7 |
| $\gamma'$ | 120 | 114 | 76 | 73 |
| $\phi_2$ | 0.85[d] | 0.79 | - | - |
| $r_{42}$ | 0.94 | 0.98 | 0.85 | 0.83 |

a Ref. 20
b Ref. 2
c Ref. 14
d Based on a predicted free-ion $F^2 = 54473\ cm^{-1}$

Table VIII. Calculated values for $g_{\Gamma_6}$

| $k^a$ | $g_{\Gamma_6}$ | $g_{exp}$ |
|---|---|---|
| 1.0 | 2.377 | |
| 0.885 | 1.896 | 1.896 [$Np(BD_4)_4$] |
| 0.862 | 1.799 | 1.799 [$Np(BH_3CH_3)_4$] |

[a] $g = \langle \psi \| k\vec{L} + g_S\vec{S} \| \psi \rangle$

Figure Captions

Figure 1. 2 K optical absorption spectra of $Np(BH_4)_4$ and $Np(BD_4)_4$ in the 2000-1500 nm region.

Figure 2. 2 K optical absorption spectra of $Np(BH_4)_4$ and $Np(BD_4)_4$ in the 1400-350 nm region.

Figure 3. EPR spectrum of $Np(BD_4)_4/Zr(BD_4)_4$ at 2 K:
(a) X-band spectrum at 9.39 GHz;
(b) K-band spectrum at 24.2 GHz.

Figure 4. Energy level diagram for a Kramer doublet with $S' = 1/2$, $I = 5/2$, $g = 1.894$, $A = 0.114\ cm^{-1}$. Allowed transitions are indicated with vertical arrows; -.-.-: X-band, ____: K-band, ——: Q-band. Q-band transitions are only indicated below 11 kGauss.

Figure 5. Inverse paramagnetic susceptibility of $Np(BH_3CH_3)_4$;
ΔΔΔ: experimental data obtained at 5 kGauss.
A: calculated considering only $^4I_{9/2}$, $B_0^4 = -1461\ cm^{-1}$, $B_0^6 = -3274\ cm^{-1}$, orbital reduction factor $k = 0.82$.
B: calculated from the parameters in Table V, first column, with no orbital reduction factor.
C: same as B, but with an orbital reduction factor $k = 0.862$.

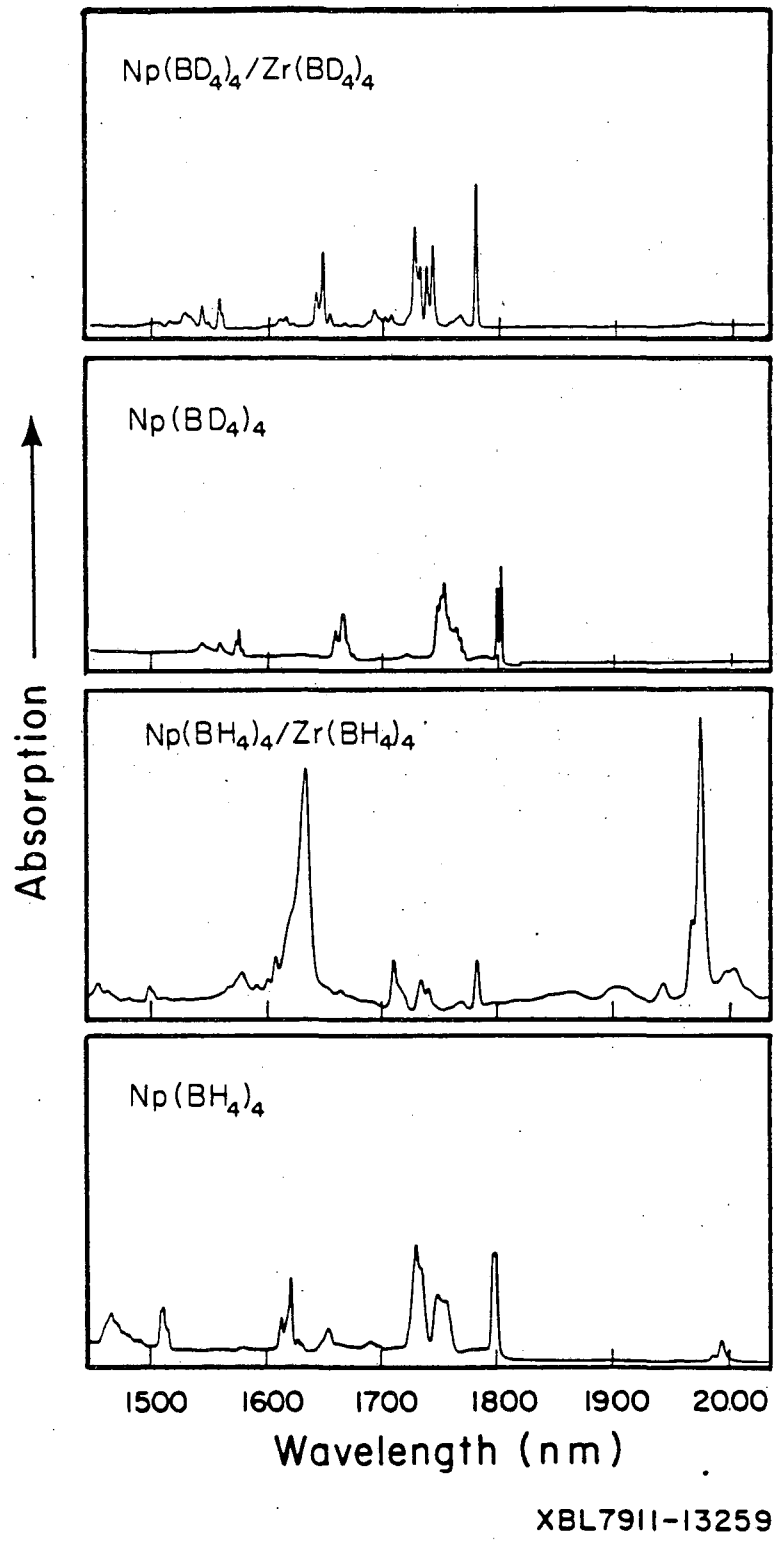
Np(BD4)4/Zr(BD4)4
Np(BD4)4
Np(BH4)4/Zr(BH4)4
Np(BH4)4
Absorption
1500
1600
1700
1800
1900
2000
Wavelength (nm)
XBL7911-13259

Figure 1

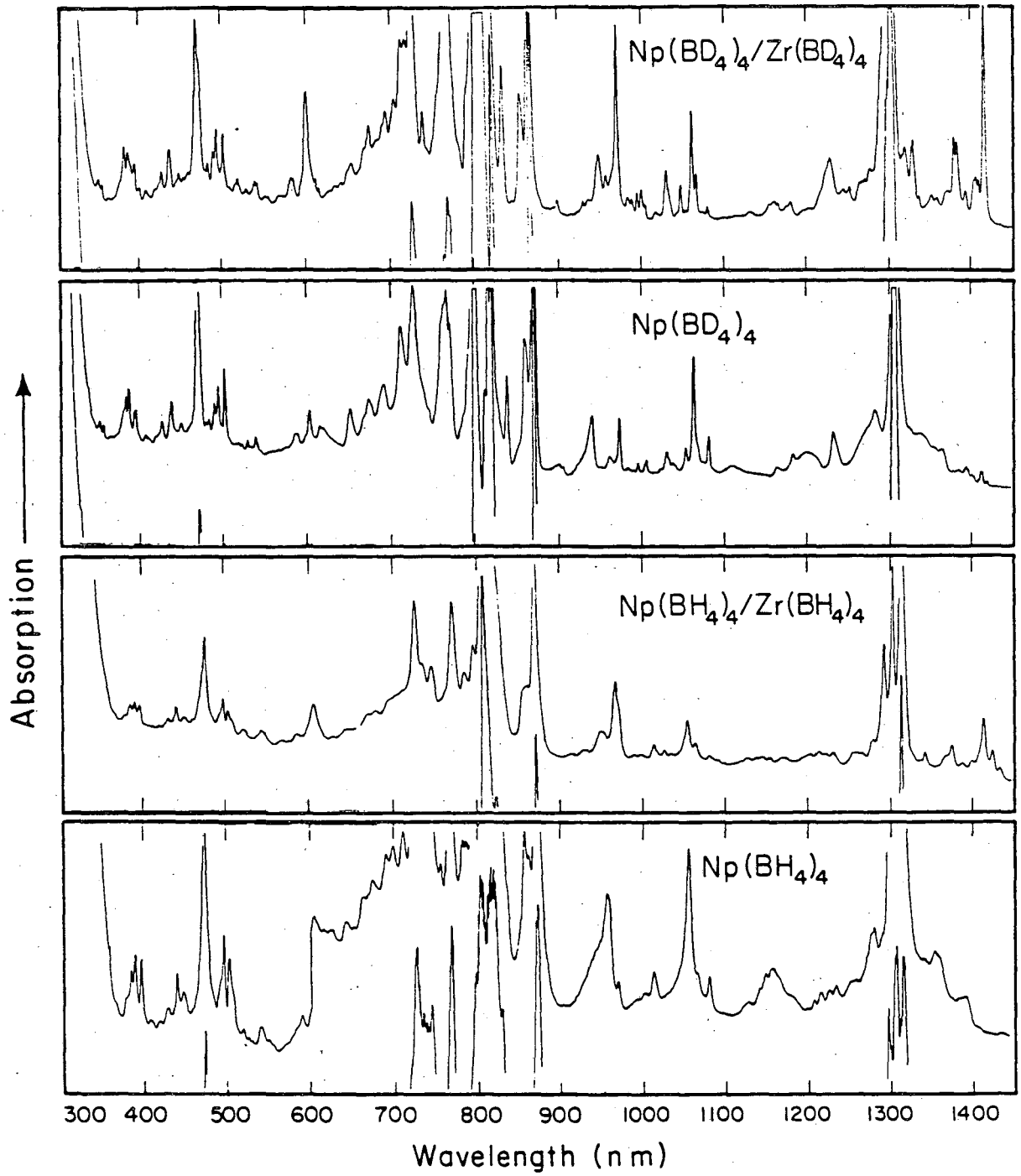
Np(BD4)4/Zr(BD4)4
Np(BD4)4
Np(BH4)4/Zr(BH4)4
Np(BH4)4
Absorption
300 400 500 600 700 800 900 1000 1100 1200 1300 1400
Wavelength (nm)
XBL 837-478

Figure 2

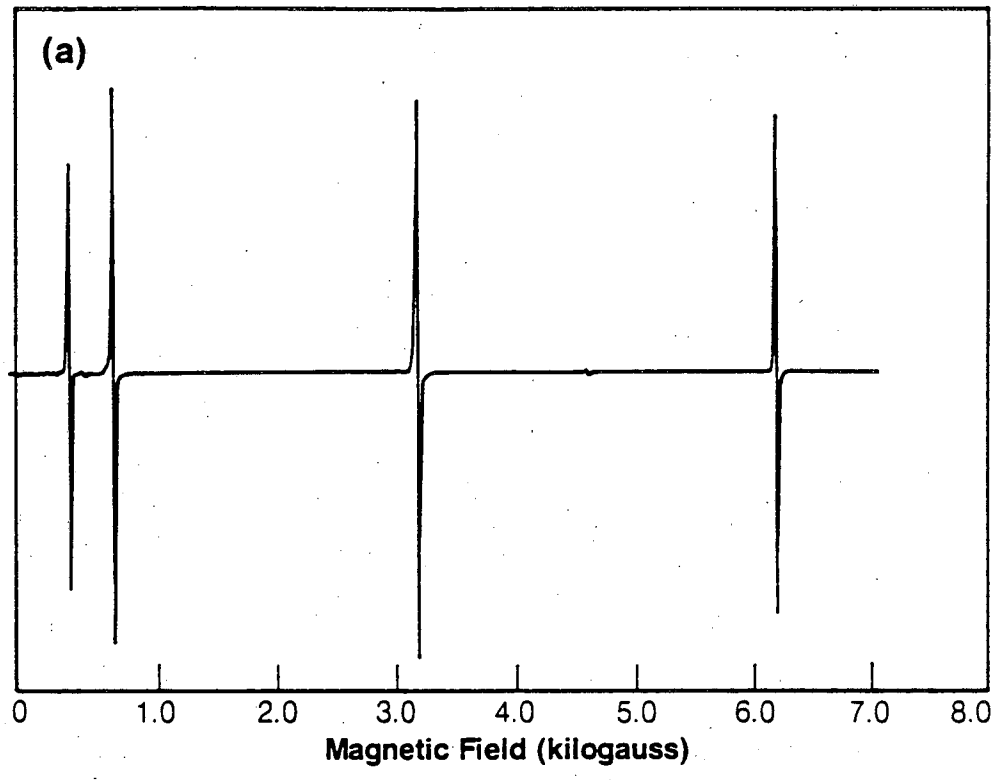


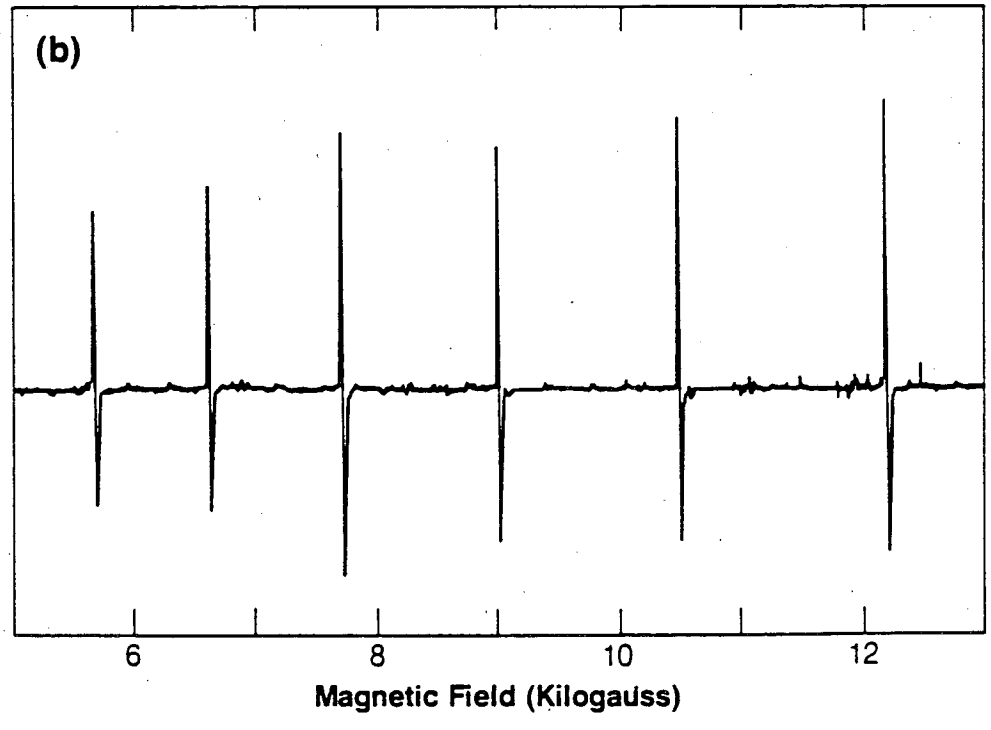


XBL 837-475

Figure 3

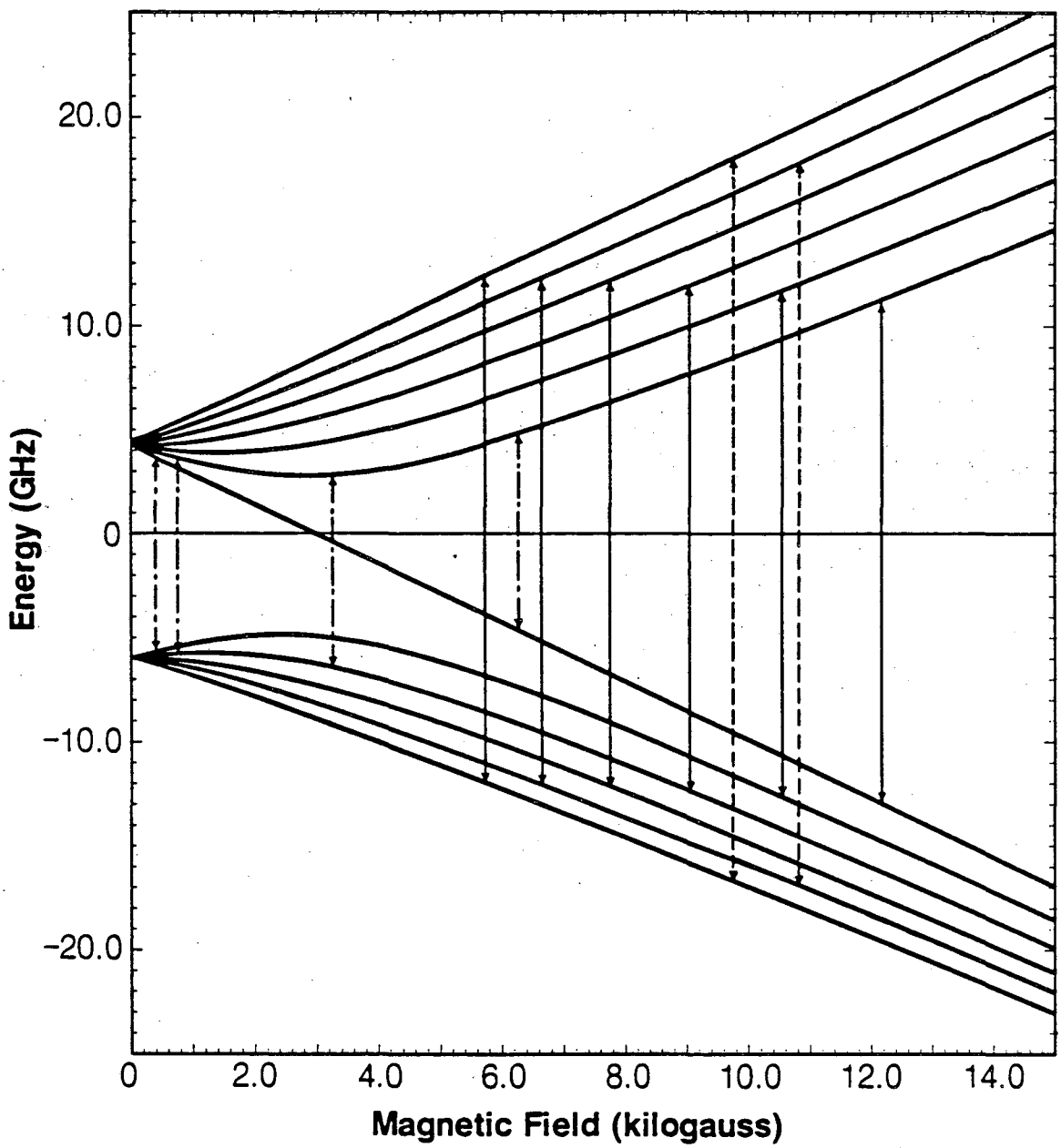
20.0
10.0
0
-10.0
-20.0
Energy (GHz)
0
2.0
4.0
6.0
8.0
10.0
12.0
14.0
Magnetic Field (kilogauss)
XBL 838-10938

Figure 4

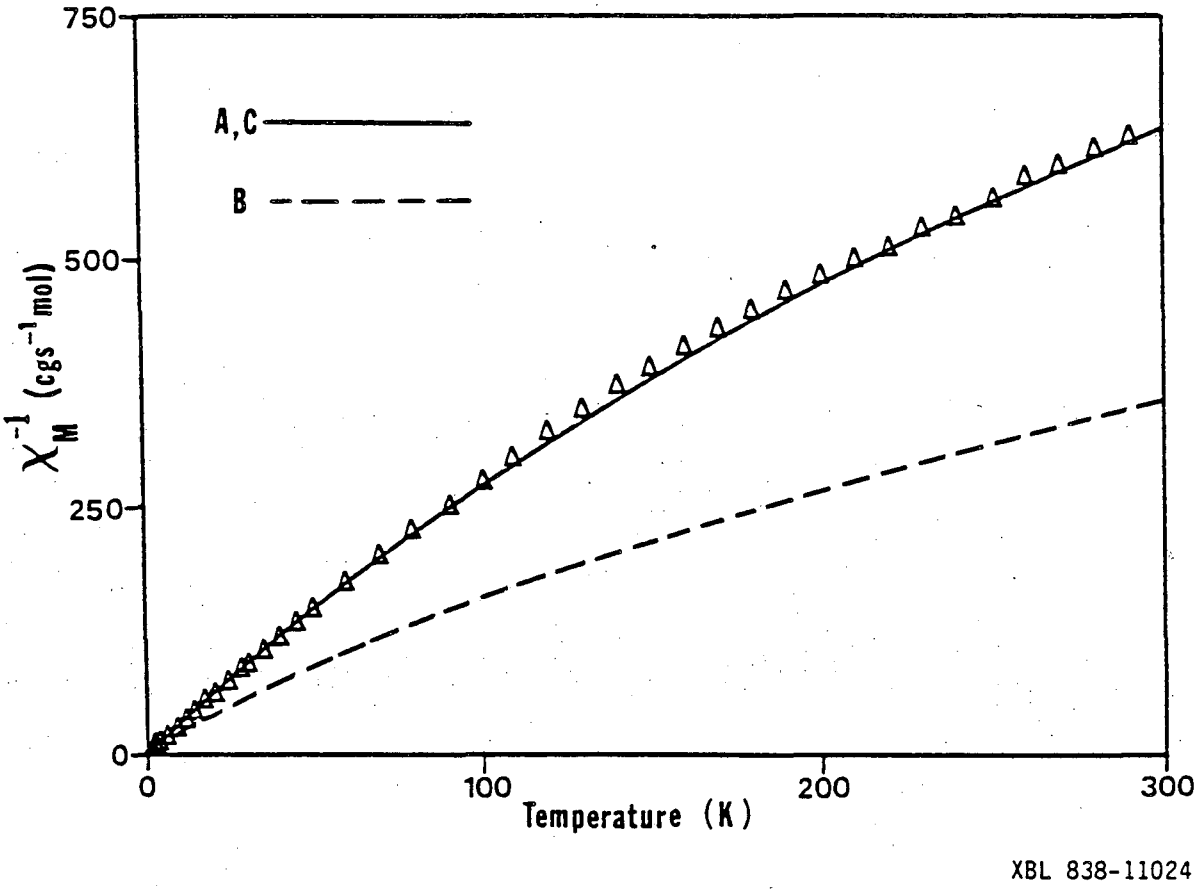
750
500
250
0
A,C
B
$\chi_M^{-1}$ (cgs$^{-1}$mol)
0
100
200
300
Temperature (K)
XBL 838-11024

Figure 5

This report was done with support from the Department of Energy. Any conclusions or opinions expressed in this report represent solely those of the author(s) and not necessarily those of The Regents of the University of California, the Lawrence Berkeley Laboratory or the Department of Energy.

Reference to a company or product name does not imply approval or recommendation of the product by the University of California or the U.S. Department of Energy to the exclusion of others that may be suitable.

*TECHNICAL INFORMATION DEPARTMENT*
*LAWRENCE BERKELEY LABORATORY*
*UNIVERSITY OF CALIFORNIA*
*BERKELEY, CALIFORNIA 94720*